

Accepted for Journal of Computational Physics, Feb 20, 2010

Numerical fluid solutions for nonlocal electron transport in hot plasmas: equivalent diffusion versus nonlocal source

Denis Colombant
Wallace Manheimer*
Plasma Physics Division
Naval Research Laboratory
Washington DC

Abstract

Flux limitation and preheat are important processes in electron transport occurring in laser produced plasmas. The proper calculation of both of these has been a subject receiving much attention over the entire lifetime of the laser fusion project. Where nonlocal transport (instead of simple single flux limit) has been modeled, it has always been with what we denote the equivalent diffusion solution, namely treating the transport as only a diffusion process. We introduce here a new approach called the nonlocal source solution and show it is numerically viable for laser produced plasmas. It turns out that the equivalent diffusion solution generally underestimates preheat. Furthermore, the advance of the temperature front, and especially the preheat, can be held up by artificial ‘thermal barriers’. The nonlocal source method of solution, on the other hand more accurately describes preheat and can stably calculate the solution for the temperature even if the heat flux is up the gradient.

* Consultant to the NRL Plasma Physics Division through RSI Corporation, Lanham, MD

Report Documentation Page			Form Approved OMB No. 0704-0188		
<p>Public reporting burden for the collection of information is estimated to average 1 hour per response, including the time for reviewing instructions, searching existing data sources, gathering and maintaining the data needed, and completing and reviewing the collection of information. Send comments regarding this burden estimate or any other aspect of this collection of information, including suggestions for reducing this burden, to Washington Headquarters Services, Directorate for Information Operations and Reports, 1215 Jefferson Davis Highway, Suite 1204, Arlington VA 22202-4302. Respondents should be aware that notwithstanding any other provision of law, no person shall be subject to a penalty for failing to comply with a collection of information if it does not display a currently valid OMB control number.</p>					
1. REPORT DATE 20 FEB 2010	2. REPORT TYPE	3. DATES COVERED 00-00-2010 to 00-00-2010			
Numerical fluid solutions for nonlocal electron transport in hot plasmas: equivalent diffusion versus nonlocal source			5a. CONTRACT NUMBER		
			5b. GRANT NUMBER		
			5c. PROGRAM ELEMENT NUMBER		
6. AUTHOR(S)			5d. PROJECT NUMBER		
			5e. TASK NUMBER		
			5f. WORK UNIT NUMBER		
7. PERFORMING ORGANIZATION NAME(S) AND ADDRESS(ES) Plasma Physics Division, Naval Research Laboratory, Washington, DC			8. PERFORMING ORGANIZATION REPORT NUMBER		
9. SPONSORING/MONITORING AGENCY NAME(S) AND ADDRESS(ES)			10. SPONSOR/MONITOR'S ACRONYM(S)		
			11. SPONSOR/MONITOR'S REPORT NUMBER(S)		
12. DISTRIBUTION/AVAILABILITY STATEMENT Approved for public release; distribution unlimited					
13. SUPPLEMENTARY NOTES					
14. ABSTRACT					
15. SUBJECT TERMS					
16. SECURITY CLASSIFICATION OF: a. REPORT b. ABSTRACT c. THIS PAGE unclassified unclassified unclassified			17. LIMITATION OF ABSTRACT Same as Report (SAR)	18. NUMBER OF PAGES 29	19a. NAME OF RESPONSIBLE PERSON

I Introduction

In a laser produced plasma, electron thermal energy is transported principally by electrons with energy between about 5 and 16 times the thermal energy. Electrons with less than 5 times the thermal energy do not transport any significant energy. Because of the Maxwellian nature of the electron distribution function, there are effectively no electron with energy greater than 16 times the thermal energy. Thus even if the mean free path of thermal electrons is smaller than the temperature gradient scale length, the mean free path of the energy carrying electrons, (which is proportional to the energy squared) may be longer, meaning the transport cannot be described strictly locally (for instance proportional to the temperature gradient).

This problem has long been recognized in laser produced plasmas. Recently we have published several papers [1-3] examining the use of a Krook model to describe nonlocal transport. Of course we are well aware of the limits of a Krook model and these have been fully discussed in Refs. [1-3]. There several independent tests of the model were made and the simulations passed these tests. Also elements of a fully conservative Krook model were sketched out [1].

Since so much of the physics of laser matter interaction is best modeled with fluid simulations, it is important to find some way of treating nonlocal flux within the constraints of a fluid model if at all possible. Alternate simulation schemes such as Fokker Planck or direct simulation Monte Carlo could, at very great expense, treat nonlocal transport more accurately, but would certainly fail for treating every other physical process, whereas a local fluid model works very well. Very briefly, Refs. [1-3] found that the electron energy flux can be split into two parts, a diffusive like part describing the low energy electrons, and a nonlocal component describing the higher energy electrons. Regarding the local part, one finds that the diffusion coefficient is reduced from classical. This is the way our Krook model handles flux limitation. The nonlocal part is expressed as an integral over particle energy and a convolution over space. It allows the hotter part of the plasma to heat the cooler parts even though these are some distance away. This is the way our Krook model describes preheat.

Others have also introduced variants of Krook models to describe the nonlocal transport [4,5]. Previously other authors have also proposed convolutions to describe the energetic particle transport, either ad hoc [6], or based on comparison to Fokker Planck solutions in infinite homogeneous plasmas [7,8].

What all of these methods have in common is that when it comes time to perform a numerical solution of the energy transport equation, they apply what we term the equivalent diffusion solution [7-9]. That is take the energy flux, however it was derived, and divide by the negative temperature gradient to get an equivalent diffusion coefficient (or more accurately an equivalent thermal conduction, which has dimension nx^2/t , where n is the electron density,

instead of a diffusion coefficient which has dimension x^2/t). Then the problem is solved as a diffusion problem. This usually makes use of an implicit numerical scheme has the advantage of being unconditionally stable. However in a laser plasma simulation the diffusion coefficient depends on temperature so the problem is nonlinear and more complicated. We discuss this further shortly. Furthermore there are problems with this approach which were apparent to its early users [7]. Namely there could be a thermal flux where the temperature gradient is zero, implying infinite equivalent diffusion coefficient. To handle this, the diffusion coefficient is limited by some maximum value, typically a thousand or a million times classical. An even more serious problem is that the flux may be up the temperature gradient rather than down it. This would mean a negative diffusion coefficient. The solution (both analytically and numerically) would be unstable. To treat this case, wherever the equivalent diffusion coefficient is negative, it is replaced with the classical positive value. This is the way nonlocal transport has been handled up to now, but there has neither been an independent check of it, nor examination of the validity of the equivalent diffusion solution.

Here we solve the nonlocal transport equation without using an equivalent diffusion solution and compare our solutions to it. We call this new technique the nonlocal source solution. The diffusive part of the transport is treated in the usual way, with an implicit solution. The nonlocal part is treated as an energy source and treated explicitly. One might think there could be problems with numerical stability. After all the code has, among other constraints, a Courant condition based on the ion or fluid velocity. However as we mentioned, the electron energy is transported by electrons with energy between about 5 and 16 times the thermal energy, so one might think such an approach would be numerically unstable. However this is usually not the case. The implicit solution of the diffusive part gives rise to a strong stabilizing effect. In Section II we work out the numerical stability condition for the nonlocal source solution. Depending on the relative sizes of the local versus nonlocal flux, there may be no instability limit at all on the time step. If the nonlocal part is sufficiently large, and the local part is sufficiently small, there is a stability condition, but the constraint is weak for typical laser plasmas.

It is interesting to compare our Krook model for transport in laser plasmas with advanced techniques for handling transport in magnetically confined plasmas [10,11]. For the former, turbulence likely does not play a major role, although it may arise in such a way that it can be modeled with an enhanced collision frequency [12,13]. Rather what is important is the nonlocal transport of the energetic particles, the local transport of the low energy particles, and their interplay. Any theory here must involve velocity space. For the magnetic fusion case, turbulence apparently plays a major role, and advanced mathematical techniques have been proposed to deal with it. However these techniques do not involve velocity space, and they are probably not appropriate for the case of laser produced plasmas.

Section III works out the stability condition for our Krook model of electron transport. This lets us evaluate the maximum stable time step and insure that the code runs with a smaller time step. In most cases we have looked at, there is, in practice, no additional constraint.

Section IV applies this to a simple problem, a uniform (i.e. infinitely massive ions) plasma with a background temperature of 1 keV, but imbedded within is a slug of 50 keV plasma. We solve for the time evolution of the temperature profile using classical thermal conductivity, Krook model using an equivalent diffusion solution, and Krook using a nonlocal source solution. For the latter we find that the numerical stability condition is well satisfied. The classical solution has a rapidly moving heat front and no evidence of preheat, as expected. The equivalent diffusion solution has a slower moving main heat front and a small amount of preheating. The nonlocal source solution has a slower moving heat front than classical, but faster than the equivalent diffusion solution. Most important, it has stronger preheat than the equivalent diffusion solution. Our conclusion is that the equivalent diffusion solution can underestimate the preheat. Also we show that the nonlocal source solution has no problem with energy flux up a temperature gradient, whereas the equivalent diffusion solution encounters artificial ‘thermal barriers’. Section V briefly reexamines the problem of a 4 keV plasma slug embedded in a 1 keV plasma. This was initially examined with a Fokker Planck simulation by Matte and Virmont [14]. In Ref. (2) we compared the equivalent diffusion solution to this problem with the Fokker Planck solution, and concluded that the Krook model compared more favorably than any other transport model, especially in the time asymptotic limit. In Section V. we examine this problem comparing the nonlocal source solution with the equivalent diffusion solution as a function of time. We find the two solutions are close, and in the time asymptotic limit approach one another. Finally Section VI gives conclusions.

II. The nonlocal source term approach and its stability

In the models for non thermal electron energy transport which we have developed [1-3], we found that the electron thermal energy flux is the sum of two terms, a local term which has the properties of classical transport, and a nonlocal term which is a convolution over space as well as an integral over energy. As the temperature equation has many terms, representing many physical processes in it, we examine the numerical stability of a simpler system, namely a temperature equation of the form

$$\frac{\partial T}{\partial t} = WD \frac{\partial^2 T}{\partial x^2} + \int_{\Xi_{cr}}^{\infty} d\Xi \left\{ \frac{\partial}{\partial x} \int dx' \frac{K(\Xi)}{2} \alpha(\Xi) \exp\{-|K(\Xi)(x - x')|\} \frac{\partial T(x')}{\partial x'} \right\} \equiv -\frac{\partial}{\partial x} (q_l + q_{nl}) \quad (1)$$

For an actual laser plasma, the situation is more complicated because D is a function of T(x) and α is a function of T(x'). However we proceed with the simple linear case and discuss its validity and applicability shortly. In an analytic theory of course, the nonlocal flux alone is sufficient. But when interpolating onto a finite spatial grid, for many energies (i.e Ξ 's) the x' integration takes place within a single grid cell. For these energies, the finite difference

approximation is not even qualitatively correct. Thus in practice, it is necessary to split the flux into a local and nonlocal part. We will discuss this in more detail shortly.

Here D is the classical diffusion coefficient, and W is the reduction from the classical result [1-3]. It arises because as nonlocal effects become more important, the local transport decreases. The second term in Eq. (1) comes from the thermal flux arising from nonlocal effects. It is an integral over particle energy Ξ . As discussed in [2,3], the minimum energy Ξ_{cr} is determined first by the condition that WD is positive (meaning $\Xi_{cr}/T > 3.5$); and second by the condition that the integral over x' is reasonably represented by the summation (meaning $K(\Xi_{cr})\Delta x < 0.2$; $K(\Xi)$ being a decreasing function of Ξ reflecting the longer mean free paths of the more energetic particles). The last terms on the right simply defines this rate of change of temperature in terms of the gradients of local and non local fluxes. As long as WD and α are positive, there are no unstable, i.e. exponentially growing solutions to Eq. (1).

In the literature [1-9], this equation has typically been solved with what we call the equivalent diffusion solution. Namely one defines an equivalent diffusion coefficient

$$D_{eq} = -\frac{q_l + q_{nl}}{\frac{\partial T}{\partial x}} \quad (2)$$

and solves the equation as a diffusion equation. However if the temperature gradient becomes zero, D_{eq} is infinite. Even more of a problem, if D_{eq} is negative in some regions, the diffusion equation is violently unstable. To treat these cases, the approach has been to restrict D_{eq} to some maximum, say 10^3 times classical, and in regions where D_{eq} is negative, to replace it with the positive classical result. We will see that this can lead to greatly inaccurate solutions in some cases.

Instead of the equivalent diffusion solution, we treat the added term in Eq. (1) as a nonlocal source term and treat it explicitly, that is in solving for the $(n+1)$ time step, the source term is evaluated at the n^{th} time step. However we treat the local diffusion term implicitly, that is the diffusion term is evaluated at the $(n+1)$ time step. If a diffusion equation is solved implicitly, there is no constraint on the time step for numerical stability, but only for accuracy. However when treating diffusion-like equations explicitly, the condition for numerical stability demands a very small time step. Indeed for the case of a grid of space step Δx and time step Δt , the well known condition for stability is (for $W=1$), $\Delta t < \Delta x^2 / 2D$.

Let us pause here to briefly discuss the implicit solution to the temperature equation as done in laser fusion calculations. If D were constant, the implicit calculation is straightforward. The problem is that D has strong temperature dependence; it varies roughly as $T^{5/2}$, with other weaker dependences as well. Each laboratory doing laser fusion calculations uses its own approach. At NRL, we use the fluid simulation code FAST [15]. It treats the implicit temperature calculation with an iteration scheme [16]. The temperature dependence of D is

expressed at the current time step and then T is advanced implicitly as a linear calculation. This new T is then used in D and the process is iterated until convergence is achieved. In practice, it works very well with a few iterations.

Hence before applying a nonlocal source term approach, we must first examine the numerical stability where the source term is treated explicitly and the diffusion term is treated implicitly. An actual numerical stability calculation, taking into account the dependence of D and α on T would be extremely complicated due to the fact that this introduces both inhomogeneity and nonlinearity. Furthermore, even if one could do such a stability calculation, it would be of little use; every temperature profile would have a different stability condition. To proceed, we do a much simpler numerical stability calculation, we consider D and α to be independent of space (but α depends on Ξ). Hence we consider only the linear homogeneous problem. Intuitively one would expect this to give reasonable guidance; such an approach is standard in the literature and goes back to a textbook on numerical methods [17]. Furthermore, we will see shortly that there are other convincing reasons to believe that the results of the stability analysis can be applied in a much more general sense.

To continue, we write out the discrete forms of the various operators. Here superscripts refer to time step, subscripts to spatial step. To examine the numerical stability, we assume that

$$T^{n+1}_p = [\exp(-v\Delta t)]T^n_p \quad (\text{i.e. } T(t) \sim \exp(-vt)) \quad (3a)$$

$$T^n_{p+1} = [\exp(-k\Delta x)]T^n_p \quad (\text{i.e. } T(x) \sim \exp(ikx)) \quad (3b)$$

Ultimately we wish to solve for the dispersion relation between v and k . Note that if $v < 0$, for the finite difference problem, whereas if $v > 0$ for the continuum problem (as it is for our case), the solution is numerically unstable.

We now write out the discrete forms of the various terms in Eq. (1). The first is

$$\frac{\partial T}{\partial t} = \frac{T^n_p \exp(-v\Delta t) - T^n_p}{\Delta t} \quad (4)$$

The second is

$$-\frac{\partial q_{l_p}}{\partial x} = WD \left\{ \frac{\exp(ik\Delta x) - 2 + \exp(-ik\Delta x)}{\Delta x^2} \right\} T^n_p \exp(-v\Delta t) \quad (5)$$

where we note here that on the right hand side of Eq. (5), T is evaluated at the advanced time step, $t = (n+1)\Delta t$. The nonlocal term on the right hand side of Eq. (1), when written in finite

difference form, and using Eq. (3b) breaks up into summations over various geometric series with ratio $\exp[(-K(\Xi)+ik)\Delta x]$ or $\exp[(-K(\Xi)-ik)\Delta x]$. Doing these sums over the geometric series, we find that this term is

$$\begin{aligned} -\frac{\partial q_{nl}}{\partial x} &= T^n p \int d\Xi \frac{K(\Xi)\alpha(\Xi)}{2\Delta x} \{ \exp(ik\Delta x) - 2 + \exp(-ik\Delta x) \} \\ &\times \left[\frac{1}{1 - \exp(-K(\Xi)\Delta x + ik\Delta x)} + \frac{\exp[(-K(\Xi) - ik)\Delta x]}{1 - \exp(-K(\Xi)\Delta x - ik\Delta x)} \right] \\ &\equiv T^n p \int d\Xi \frac{K(\Xi)\alpha(\Xi)}{2\Delta x} \{ \exp(ik\Delta x) - 2 + \exp(-ik\Delta x) \} R(K(\Xi)\Delta x, k\Delta x) \end{aligned} \quad (6)$$

Hence we find that the dispersion relation is

$$\frac{\exp(-v\Delta t) - 1}{\Delta t} = \{ \exp(ik\Delta x) - 2 + \exp(-ik\Delta x) \} \left[\frac{WD \exp(-v\Delta t)}{\Delta x^2} + \int d\Xi \frac{K(\Xi)\alpha(\Xi)}{2\Delta x} R(K(\Xi)\Delta x, k\Delta x) \right] \quad (7)$$

As is usually the case in investigations of numerical stability [17], and as we find by an investigation of Eq.(7), the most unstable wave number satisfies $k\Delta x = \pi$. To show this, the only term in Eq. (7) which can drive instability is the R term, the nonlocal term. The numerical solution will first exhibit instability where this term maximizes. By manipulating the expression for R , and using the half angle formula, it is possible to show that each term in the Ξ summation has for its $k\Delta x$ dependence

$$\frac{1 - \cos k\Delta x}{A(\Xi) - \cos k\Delta x}$$

where $A(\Xi)$ is a function of Ξ which is not necessary to write out for our purposes here except to note that is always greater than one. Clear this maximizes at $k\Delta x = \pi$, meaning that the numerical scheme is first unstable for this wave number.

Let us now reconsider the linear homogeneous approximation used in the stability analysis. Even though the temperature varies in x , there is rarely very much temperature variation within a few grid cells. However numerical instability occurs on the very shortest spatial scale length, so the background appears nearly homogeneous. Thus the approximation of constant D , where the local temperature used in D is regarded as a constant local value is reasonably valid.

Taking $k\Delta x = \pi$, we find

$$R(K(\Xi)\Delta x, \pi) = \frac{1 - \exp(-K(\Xi)\Delta x)}{1 + \exp(-K(\Xi)\Delta x)} \approx \frac{K(\Xi)\Delta x}{2} \quad (8)$$

We assume here that $k(\Xi)\Delta x \ll 1$. For those energies for which $k\Delta x \gg 1$, expressing the Δx integral in Eq. (1) as a finite summation, as in deriving Eq.(6) is not even qualitatively correct. For these energies for which $k(\Xi)\Delta x \gg 1$, the energy flux is treated with the local approximation. In treating the energy flux in for instance a laser produced plasma, there is a very wide range of particle energies, say from $\Xi = 10\text{eV}$ to $\Xi = 100\text{keV}$. Since the mean free path, proportional to Ξ^{-2} varies over 8 orders of magnitude, and since a laser plasma simulation typically has fewer than 1000 spatial cells, flux cannot be treated either all locally or all nonlocally (unless the most energetic electron has mean free path less than a grid cell).

Let us illustrate this point with a simple example. Say the plasma temperature is 1 keV and the mean free path of a 2 keV electron is one grid cell. In practice, we find that due to the Maxwellian nature of the distribution function, there is no contribution to the thermal flux from energies above 16 times the temperature [1]. Since the mean free path is proportional to the temperature squared, this means that the most energetic electron spreads out its energy over 64 grid cells. Clearly this must be treated nonlocally. On the other hand, there are also many electrons with energy of for instance 500 eV. These deposit their energy in 1/16 of a grid cell. Clearly any numerical algorithm which has them spreading their energy out over many grid cells will be incorrect. Thus given the constraints of a finite grid, one has no choice but to break up the energy range into two regimes, the lower energies treated locally, the higher, nonlocally.

We find that a good approximation is to treat the electron flux nonlocally if its mean free path is five grid cells (i.e $k\Delta\xi < 0.2$) or longer [3].

So the dispersion relation for this $k\Delta x$ is

$$\exp(-v\Delta t) = \frac{1 - A\Delta t}{1 + 4WD\Delta t/\Delta x^2}, \quad \text{with} \quad A = \int_{\Xi_{cr}}^{\infty} d\Xi K^2(\Xi) \alpha(\Xi) \quad (9)$$

The condition for numerical instability is that the right hand side of Eq(9) has a magnitude greater than unity. Since the sign in this case is negative, this means that for numerical instability, we need $\text{Re } v < 0$ and $\text{Im } v = \pi$. Hence the condition for numerical instability is

$$A\Delta t > 2 + \frac{4WD\Delta t}{\Delta x^2} \quad (10)$$

As long as $A < 4WD/\Delta x^2$, solving the local diffusion part implicitly, and the nonlocal source term explicitly, will always be numerically stable. In other words the natural stability of the

implicit solution of the solution of the diffusion equation will always overpower the tendency of the explicit solution of the nonlocal source term toward stability. This is a numerical condition involving only Δx , and not Δt . On the other hand, if $A > 4WD/\Delta x^2$, we find numerical stability as long as the time step satisfies the condition

$$\frac{\Delta t}{\Delta t_{ex}} < \frac{1}{A\Delta t_{ex}/2 - W} \quad (11)$$

Here Δt_{ex} is the maximum time step for stability for the explicit diffusion calculation, $\Delta x^2/2D$. This is plotted graphically in Fig (1). *In this case, the stability condition once again depends on Δt .*

III. Calculation of $\alpha(\Xi)$ and the numerical stability condition for a laser produced plasma.

In our earlier work, we have written out expressions for the thermal flux using a Krook model for electron electron collisions and a Fokker Planck model for electron ion collisions [1-3]. There the electron ion and electron collision frequencies were

$$\nu_{ee} = \frac{5.8 \times 10^{-6} n \Lambda}{T_e^{3/2} \left[1 + (5.8/7.7) (\Xi/T)^{3/2} \right]} \equiv \frac{2\nu_e}{\left[1 + (5.8/7.7) (\Xi/T)^{3/2} \right]} \equiv \nu_e S(\Xi, Z) \quad (12)$$

$$\nu_{ei} = 1.34 Z \nu_e \left(mv^2 / 2T \right)^{-3/2} \equiv \nu_e S_i(\Xi, Z) \quad (13)$$

$$\nu_{ei} + \nu_{ee} = \nu_e S(v, Z) \quad (14)$$

Notice that these collision frequencies are functions of particle energy Ξ , as well as position through the spatial dependence of the electron density n , the Coulomb logarithm Λ , the electron temperature T , and the charge state Z .

In Refs. [1-3] we derived an expression for the energy flux:

$$q(x) = -K_{sp} T^{5/2} T' \left[\frac{\beta(\Xi_{cr}(r)/T(x))}{\beta(\infty)} + 0.92 \frac{Z_4 R(\Xi_{cr}(x)/T(x))}{Z_2 \beta(\infty)} \right] - \frac{\Lambda(x) K_{sp}(x)}{2\beta(\infty)} \int_{\Xi_{cr}}^{\infty} d\Xi \int_{-\infty}^{\infty} dr' \left[1 - 0.92 \frac{Z_4(x) T(x)}{Z_2(x) \Xi} \right] \Pi_{zc}(x, x', \Xi) \equiv q_L(x) + q_{NL}(x) \quad (15)$$

where q_L and q_{NL} are the local and nonlocal terms in $q(x)$ and

$$\Pi_{zc}(x, x', \Xi) = \frac{K(x', \Xi) \Xi^4 \left\{ \frac{\Xi}{T(x')} - \frac{Z_4(x)}{Z_2(x')} \right\} \exp\{-[\Xi/T(x')]\} \exp\{-|H(x, x' \Xi)|\}}{\Lambda(r') T_e(r')^{5/2} \{1 + Z(r')/2\}} \frac{\partial T_e(x')}{\partial x'} \quad (16)$$

Other quantities in Eq. (15) are

$$\beta(y) = \int_0^y du u^{5/2} \frac{\{u - Z_4/Z_2\}}{S(u)} \exp(-u) \quad (17)$$

$$R(y) = \int_y^\infty du \frac{u^{3/2} \left\{ u - \frac{Z_4}{Z_2} \right\}}{S(u)} \exp(-u) \quad (18)$$

$$Z_n(Z) = \int_0^\infty u^n du u^n \frac{\exp(-u^2)}{S(u, Z)} \quad (19)$$

Analytic approximations to these quantities have been given elsewhere (1-3). We note that in the analytic approximations, the Z dependence is only meaningful if $Z > 1$. However the colder regions of a laser produced plasma are not necessarily fully ionized. In these regions, we use the analytic expressions, but evaluate them at $Z=1$. Regarding the nonlocal transport, these cold unionized or partially ionized regions play no role as a source of energetic electrons, but of course they can be important as regards other physical effects.

The quantity H is given by

$$H(x, x', \Xi) = \int_{x'}^x dx'' K(x'', \Xi) \quad (20)$$

where

$$K(r, \Xi) = \frac{\sqrt{3\nu_{ee}(r, \Xi)[\nu_{ee}(r, \Xi) + \nu_{ei}(r, \Xi)]}}{6 \times 10^7 \Xi^{1/2}} \quad (21)$$

And K_{sp} is the Spitzer conductivity

$$K_{sp} = \frac{3.1 \times 10^{10}}{\Lambda} \times \frac{0.4(Z + 0.235)}{Z + 4.242} \quad (22)$$

and the expression for Ξ_{cr} , from Refs. (2 and 3) is

$$\Xi_{cr}(x) = \text{Max} \left\{ 5T_e(x), \text{Min} \left[\begin{array}{l} (1.15 \times 10^{-12} n(x) \Lambda(x) (1 + Z(x)/2) \Delta x)^{1/2}, \\ (2.03 \times 10^{-13} n(x) \Lambda(x) (1 + Z(x)/2) L_T)^{1/2} \end{array} \right] \right\} \quad (23)$$

In Equations (12 -23), all quantities are in cgs units except energies, (Ξ and T) which are in electron volts. Since the flux is the energy flux, to write the equation in terms of diffusion equation for temperature, we must divide the flux by the specific heat C_v , which in the case of a fully ionized plasma is $3n/2$.

Hence the dimensionless quantity W is given by

$$W(\Xi_{cr}(x)/T_e(x)) = \frac{\beta(\Xi_{cr}(x)/T(x))}{\beta(\infty)} + 0.92 \frac{Z_4 R(\Xi_{cr}(x)/T(x))}{Z_2 \beta(\infty)} \quad (24)$$

As shown in Ref. (3), W(u) need be evaluated only for $5 < u < 14$. It varies (monotonically increasing) from about 0.125 at $u=5$ to unity for $u=14$ and above. Because $W < 1$ where nonlocal transport occurs, the flux due to the ‘local’ transport is reduced.

As explained in Refs. (1- 3), Ξ_{cr} is the critical energy dividing the low energy electrons, with short mean free path, which must be treated locally; from the higher energy, long mean free path electrons which must be treated nonlocally. As discussed in Refs. (2 and 3), this depends on the size of the grid cell Δx . This is a consequence of the rather small number of total grid cells (several hundred) to describe a range of mean free paths extending over a range of a factor of more than 10^8 in lengths. However there is an additional consideration, namely $\Xi_{cr}/T > 5$. We discuss further the consequences of this choice in the Appendix.

A laser produced plasma is extremely inhomogeneous. However in the stability calculation in the last section, we assumed a homogeneous system. But the numerical stability is determined at the shortest wavelength, $k\Delta x = \pi$. Hence as regards the stability calculation, we may consider the system to be homogeneous, so

$$H = K(x, \Xi)[x - x'] \quad (25)$$

and

$$\alpha(\Xi) = \frac{2}{3n} \left\{ \frac{K_{sp}}{\beta(\infty)} \left[1 - 0.92 \frac{Z_4 T}{Z_2 \Xi} \right] \left(\frac{\Xi^4 \left[\frac{\Xi}{T} - \frac{Z_2}{Z_2} \right] \exp\left(-\frac{\Xi}{T}\right)}{T^{5/2} [1 + Z/2]} \right) \right\} \quad (26)$$

Here all quantities are defined as a function of x (recall Ξ_{cr} is a function of x) and Ξ .

To find A , the quantity used in the stability condition, the integral of $K^2(\Xi)\alpha(\Xi)$ must be carried out from Ξ_{cr} to infinity. Since K^2 is proportional to Ξ^{-4} , this integral is particularly simple to perform analytically; however to get a simple analytic expression, one must make an asymptotic approximation to the part of the total integral which goes as $x^{-1}e^{-x}$.

Doing the Ξ integrals, we find

$$A = \frac{3.3 \times 10^{-26} n \Lambda^2 K_{sp}}{\beta(\infty) T^{5/2}} \exp\left(-\frac{\Xi_{cr}}{T}\right) \left\{ \frac{\Xi_{cr}}{T} + 1 - 1.9 \frac{Z_4}{Z_2} + 0.92 \left(\frac{Z_4}{Z_2} \right)^2 \frac{T}{\Xi_{cr}} \right\} \quad (27)$$

Thus using the spatially dependent expressions for A and W appropriate for a laser produced plasma, we can determine the maximum stable time step for stability in any such simulation. This is then added to the constraints on the time step.

IV. A sample calculation: Failure modes of the equivalent diffusion solution

Here we compare the nonlocal source term solution and the equivalent diffusion solution for a simple test problem. A uniform deuterium plasma, with electron density $8 \times 10^{23} \text{ cm}^{-3}$ and $Z=1$ is set up over a region of 0.5 cm. On the leftmost 0.05 cm, the temperature is 55 keV. Over 0.03 cm, the temperature drops to 1keV. For $x > 0.08$ cm, the initial temperature is constant at 1keV. Λ increases monotonically with temperature from 3.4 at 1 keV to 7.3 at 55 keV. This temperature profile is set up at $t=0$. The left boundary is maintained at 55 keV, while the temperature gradient is taken as zero on the right boundary. If the nonlocal expression for the flux here is not zero, the equivalent diffusion model would give an infinite diffusivity. However this has little effect on the calculation and is treated by the maximum D discussed in the introduction. A much more complete discussion of boundary conditions is given in Ref. [3]. The time and space dependence of the temperature is followed using a variety of transport models. This problem is rather like that examined by Matte and Virmont [14], and discussed in [2], except that here, there is a much greater range of temperature variation, i.e. over a factor of 50. The mean free path (i.e. K^{-1}) of a 100 keV electron is about 0.011 cm. The temperature diffusion equation is solved by breaking the region into a grid of 128 spatial

steps. In all cases, we find that the time step is stable as specified in Section II using the evaluations of A and W as spelled out in Section III.

The solution using pure Spitzer (classical conductivity) is shown in Fig (2). Because the thermal diffusion coefficient is proportional to $T^{5/2}$, the implicit procedure is not as simple as indicated in Section II. This temperature must also be evaluated at the advanced time step, and there is no simple way to do this. Accordingly all implicit schemes in laser plasma simulations initially take $T^{5/2}$ at the previous time step where it is known, and use an iteration process to converge to the proper implicit result. The time interval between the different temperature profiles is 600 ps. In Fig (3a) is shown the corresponding plots for the solution using the equivalent diffusion solution. Because W is less than unity, most of the front moves slower than it does for the classical case. However there is some preheating that is apparent.

In Fig (3b) is shown the solution using the nonlocal source solution. Again the main front moves outward noticeably slower than in the classical calculation, but faster than for the equivalent diffusion solution. However now there is noticeably more preheat. One might think that in the equivalent diffusion solution, we simply did not let the maximum diffusion coefficient be large enough, but this is not the case. We did this calculation where the maximum diffusion coefficient was limited to 10^3 , 10^6 , and 10^9 times classical, and there was virtually no difference between the results.

The reason for so much less preheat in the equivalent diffusion calculation seems to be that here, the preheating is modeled as a diffusion process, so to get from point a to point b, the energy has to pass through all points in between at whatever the maximum diffusion speed is. However in the nonlocal source solution, heating from the energetic electrons is virtually instantaneous, at least on the time scale of the electron-electron collision time ($\sim 10^{-12}$ sec for a 100 keV electron). Thus the equivalent diffusion solution does deemphasize preheat as compared to the nonlocal source solution.

The role of preheat can be illustrated more clearly by examining a third possible solution. In Fig. (3c) is shown the result of the nonlocal source solution, but where the nonlocal part is itself artificially set to zero. This is equal to the equivalent diffusion solution where the nonlocal source is also set equal to zero. We see that as in the Spitzer case, there is no preheat at all, and the main heat front advances even more slowly than in Fig. (3a). Thus the following rather complicated picture emerges. In all cases, the main front advances more slowly than it does for classical thermal conduction. This is due to flux limitation, characterized by the fact that $W(u)$, from Eq. (23) is less than unity. We can then regard going from Fig (3c to 3a to 3b) as adding more and more preheat. We see that the effect of preheat is twofold. First there is the preheat itself. However secondly, the preheat increases the temperature just ahead of the temperature front. This increases the ‘local’ flux there and speeds up the advance of the main front. Thus preheat contributes significantly to pulling the main temperature front forward.

Another failure mode of the equivalent diffusion model can be shown even more strikingly and clearly. It results from the fact that where the flux is up the gradient, the equivalent diffusion model replaces the flux with the classical flux, which may be much smaller and has the opposite sign. Instead of an initially uniform temperature of 1keV from 0.08 to 0.5 cm, let the temperature decrease linearly in space from 1keV at 0.08 cm to 500 eV at 0.3 cm, and then rise linearly to 1keV again at 0.5 cm. As far as the nonlocal flux is concerned, it is outward, and barely notices the small temperature dip and rise. However the equivalent diffusion solution sees a flux up the temperature gradient for $x>0.3$ cm, and to maintain numerical stability, it replaces the nonlocal flux up the temperature gradient with the much, much smaller classical flux down the gradient. In the equivalent diffusion model this temperature dip presents a thermal barrier, the heat cannot get to the other side without first diffusing through a region where the temperature gradient is very small, i.e. before filling in the dip.

Figure (4a and b) show the temperature profiles as a function of time for the equivalent diffusion solution (4a) and for the nonlocal source solution (4b). Notice that the initial dip and rise in temperature is hardly visible on the scale shown. However the equivalent diffusion solution hangs up around the temperature minimum whereas the nonlocal source solution does not. This is even more apparent in a blown up temperature scale shown in Fig. (5a and b). The equivalent diffusion solution (5a) clearly hangs up around the temperature minimum and cannot get by it for quite some time. The nonlocal source solution (5b) however easily overrides the temperature dip and gets past it in a very short time.

Notice that even though the energy flux is going up, rather than down a temperature gradient, the calculation is stable. This is as determined in Section II; we have checked that the time step is always below the stability threshold.

To see in more detail the effect of this thermal barrier, we compare the equivalent diffusion solution for the case where there is, and is not, a temperature dip. Figure 6 shows blow ups plots of the temperature profile at times 0.29, 1.49, 2.69, and 3.88 ns. The dotted curves are calculations with no initial temperature dip; the solid curves are as in Fig. 5. The main temperature front advances somewhat more slowly for the case with the initial temperature dip. However the greatest difference is in the preheat. For no initial temperature dip, we see significant preheat, but not nearly as much as for the equivalent source solution. However for the case of the initial temperature dip, where on the right hand side of the dip, the diffusion is classical and to the left, there is virtually no preheat.

To test the accuracy of our numerical scheme, we reran the case of Fig (3b), the nonlocal source solution, on two different spatial grids. First we took our standard case of 128 grid cells, and then we took 256 grid cells. Here the maximum temperature was taken as 45 keV instead of 55. A plot of the position of the advancing front, defined as the position of maximum curvature of the $T(x)$ graph, as a function of time is shown in Fig 7. Clearly to within an accuracy of a few percent, the results are independent of grid size.

To summarize, the equivalent diffusion solution unphysically reduces the effect of preheat as compared to the more accurate nonlocal source solution. Furthermore, it is susceptible to additional inaccurate results because artificial thermal barriers can be set up.

V. A reexamination of the Matte Virmont Fokker Planck solution.

In Ref. (2) we compared the Krook solution to that of Matte and Virmont [14]. They used a Fokker Planck code to examine the evolution of a temperature profile which starts out at 4 keV on the left boundary and drops sharply to 1 keV. Initially the 1 keV temperature is constant to the right hand boundary. For the plasma in Ref. (10), $Z=6$, the electron density is $n = 6 \times 10^{22} \text{ cm}^{-3}$, the time τ is measured in collision times for a particle at the average temperature, and the length L is measured in units of mean free path lengths for this particle. The particular simulation done here is for an $L=20$, which for our system is 0.00165 cm. Figure 8 shows the results of the equivalent diffusion solution (solid) and nonlocal source solution (dashed) as the time increases. The single solid curve is the initial temperature. Clearly the two solution methods are reasonably close to each other for this problem, but in the transient regime, the nonlocal source solution shows somewhat more preheat. In the time asymptotic limit, the two solutions are virtually the same and match well to the time asymptotic Fokker Planck solution as discussed in Ref. (2).

VI. Conclusions

In using a nonlocal transport model, we find that it is not necessary to use an equivalent diffusion solution to the energy transport equation. The new method, called the nonlocal source solution, relies on splitting the expression for the heat flux into a Spitzer like term, proportional to minus the temperature gradient, and a nonlocal source term. We have investigated the numerical stability and found that it usually allows time steps comparable to time step constraints already in the code. Thus using a nonlocal source solution, numerical stability can be maintained. The Spitzer like term is treated implicitly. The implicit treatment requires that the nonlinear nature of the diffusion equation be properly treated, as discussed in Sections II and IV. We find that the equivalent diffusion solution underestimates the effect of preheat as compared to the more accurate nonlocal source solution. Furthermore, preheat as calculated by equivalent diffusion solution is susceptible to be further underestimated if there is a thermal barrier, namely a region where the actual energy flux goes up the temperature gradient. As long as the time step obeys the stability condition, the nonlocal source solution is not held up at all by the thermal barrier, and the solution can be stably calculated even if the flux is up the gradient. However if the nonlocal source algorithm requires too small a time step, the equivalent diffusion model can in most cases be a reasonable substitute.

Appendix:

Here we investigate further the physical reason for, and the consequences of choosing $\Xi_{\text{cr}}/T > 5$. A plot of $W(u)$ is shown in Fig (A1). Notice that for $u < 3.5$, $W(u) < 0$. This is a consequence of the fact that as energetic particles carry heat and current forward, the less energetic particles must carry current backwards so that the total current is zero.

Hence if $\Xi_{\text{cr}}/T < 3.5$, the local diffusion coefficient is negative. While Eq. (10) indicates that it is possible that the algorithm be stable in this case, we find that in practice, this is rarely the case. We have solved the 50keV slug problem using the nonlocal source solution and taking $\Xi_{\text{cr}}/T = 3$. It turns out that there is a large enough region in space where the local diffusion coefficient is sufficiently negative that the code crashes. Thus in practice, using the nonlocal source solution, to maintain numerical stability, we cannot let Ξ_{cr}/T go below 3.5.

The goal then is to take the minimum value of Ξ_{cr}/T as small as possible, so that as many particles as possible can be treated nonlocally. However we must maintain numerical stability also. To us, a minimum value of 5 seems a reasonable choice. The result is not very sensitive to this choice as long as Ξ_{cr}/T remains small and numerical stability is maintained. In Fig. (A2) are shown solutions to the 50 keV slug problem at time $t = 3\text{ns}$ for several cases, Krook model nonlocal source solution with $\Xi_{\text{cr}}/T = 4$ and 5, Spitzer conductivity, and flux limited diffusion with a flux limit of 0.06. Notice that even for Ξ_{cr}/T as small as 4, stability is maintained and the solution is not very different from that with $\Xi_{\text{cr}} > 5$. These two solutions are much closer to one another than they are to either classical or flux limited transport.

Acknowledgement: This work was supported by U.S. DOE/NNSA. We would like to thank Dr. Steven Obenschain both for his continued support and encouragement, and for suggesting to us that we examine the equivalent diffusion model and see whether one can avoid using it. Also we thank Dr. Michel Busquet for helpful discussions.

References:

1. W. Manheimer, D. Colombant and V. Goncharov, Phys. Plasmas, **15**, 083103, 2008
2. D. Colombant and W. Manheimer, Phys. Plasmas, **15**, 083104, 2008
3. D. Colombant and W. Manheimer, Phys. Plasmas, **16**, 0627051, 2009
4. V. Goncharov, O. Gotchev, E. Vianello, T.. Boehly, J. Knauer, P. McKenty, P. Radha, S. Regan, T. Sangster, S. Skupsky, W. Smalyuk, R. Betti, R. McCrory, D. Meyerhoffer and C. Cherfils-Clerouin, Phys. Plasmas, **13**, 012702, 2006
5. V. Goncharov, T. Sangster , P. Radha, R. Betti , T. Boehly, B. Collins, R. Craxton, J. Delettrez, R. Epstgein, V. Glebov, S. Hu, I. Igumenshchev, J. Knauer, S. Loucks, J. Marozas, F. Marshall, R. McCrory, P. McKenty, D. Meyerhoffer, S. Regan, W. Seka, S. Skupsky, V. Smalyuk, J. Soures, C. Stoeckl, D. Schvarts, J. Frenje, R. Petraso, C. Li, F. Seguin, W. Manheimer, and D. Colombant, Phys. Plasmas, **15**, 056310, 2008
6. J.F. Luciani, P. Mora, and J. Virmont, Phys. Rev. Lett. **51**, 1664, 1983
7. E.M. Epperlein and R. Short, Phys. Fluids, **B3**, 3092, 1991
8. G.P. Schurtz, P.D. Nicolai, and M. Busquet, Phys. Plasmas, **7**, 4238, 2000
9. P.A. Holstein, J. Delettrez, S. Skupsky, and J. P. Matte, J. Appl. Phys. **60**, 2296, 1986
10. E.D. Held, J.D. Callen, C.C. Hegna, C.R. Sovinec, T.A. Gianakon, and S.E. Kruger, Phys. Plasmas, **11**, 2419, 2004
11. D. del-Castillo-Negrete, Phys. Plasmas, **13**, 082308, 2006
12. W.M. Manheimer, Phys. Fluids, **20**, 265, 1977
13. W.M. Manheimer, D.G. Colombant and B.H. Ripin, Phys. Rev. Let. **38**, 1137, 1977
14. J.P. Matte and J. Virmont, Phys. Rev. Let., **49**, 1936, 1982
15. J.H. Gardner, A.J. Schmitt, J.P. Dahlburg, C.J. Pawley, S.E. Bodner, S.P. Obenschain, V. Serlin, and Y. Aglitskiy Phys. Plasmas **5**, 1935, 1998
16. J.P. Dahlburg, D.E. Fyfe, J.H. Gardner, S.W. Haan, S.E. Bodner, and G.D. Doolen, Phys. Plasmas, **2**, 2453, 1995

17. R. Richtmeyer and K. Morton, *Difference Methods for Initial Value Problems*, p. 187,
Interscience Publishers, New York, 1967

Figure captions:

Figure 1: A plot of the stable region as a function of β ($\equiv A\Delta t_{ex}/W$) where Δt_{ex} is the explicit stable time step. Notice that if $\beta < 1$ the numerical algorithm is always stable.

Figure 2: Solution for the temperature as a function of time and space using only classical conductivity. The heat front advances quickly, but there is no preheating. The time between the curves is 600ps.

Figure 3: a) As in Fig. 2, but using the equivalent diffusion solution for the Krook model. Notice that the main front now advances more slowly and there is some preheat. b) As in Fig 2, but using the nonlocal source solution. There is now noticeably more preheat. c) As in Figs (3a and b) but where the nonlocal contribution to the flux is artificially suppressed.

Figure 4: a) The Krook model using an equivalent diffusion model where the low temperature part of the profile has an initial temperature dip. Notice that the heat front has difficulty getting past the temperature dip. b) Using the equivalent source solution. Notice that the temperature profile easily glides over the temperature dip.

Figure 5: A blown up version of Fig. 4 showing a) the difficulty the front has advancing past the temperature dip using the equivalent diffusion solution, and b) the ease with which the temperature front sweeps over the dip using the nonlocal source solution. The fact that the flux is up the gradient does not give rise to any numerical difficulty.

Figure 6: A blow up like Fig 5. for the equivalent diffusion model with and without an initial temperature dip. The graphs are at times 0.29, 1.49, 2.69, and 3.88 ns. Notice that there is no preheat in the positive gradient region.

Figure 7: A plot of the position of the advancing temperature front as a function of time for two different grids, 128 and 256 cells.

Figure 8: A plot of the temperature profile using the equivalent diffusion solution (solid) and nonlocal source solution (dashed) for the plasma studied in Refs. (2 and 10). The single solid curve is the initial temperature profile.

Figure A1: A plot of the function $W(u)$ as a function of u . Notice that for $u < 3.5$, $W(u) < 0$.

Figure A2: A plot of the temperature as a function of position at a time of 3 ns for the 50 keV slug problem discussed in Sec IV. We examine the effect of the choice of u_{min} ($= \Xi_{cr}/T$). Notice that while the solutions for $u_{min} = 4$ and 5 do not exactly overlap, they are much closer to one another than they are to either classical or flux limited transport.

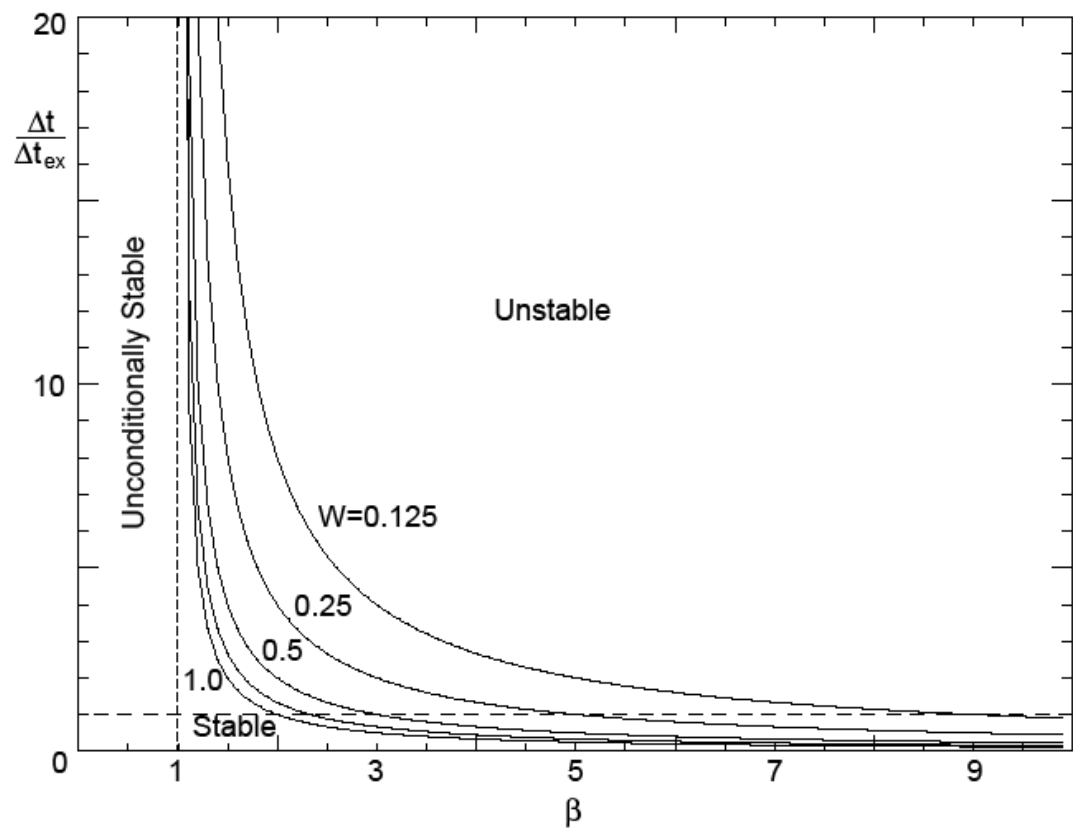


Fig.1

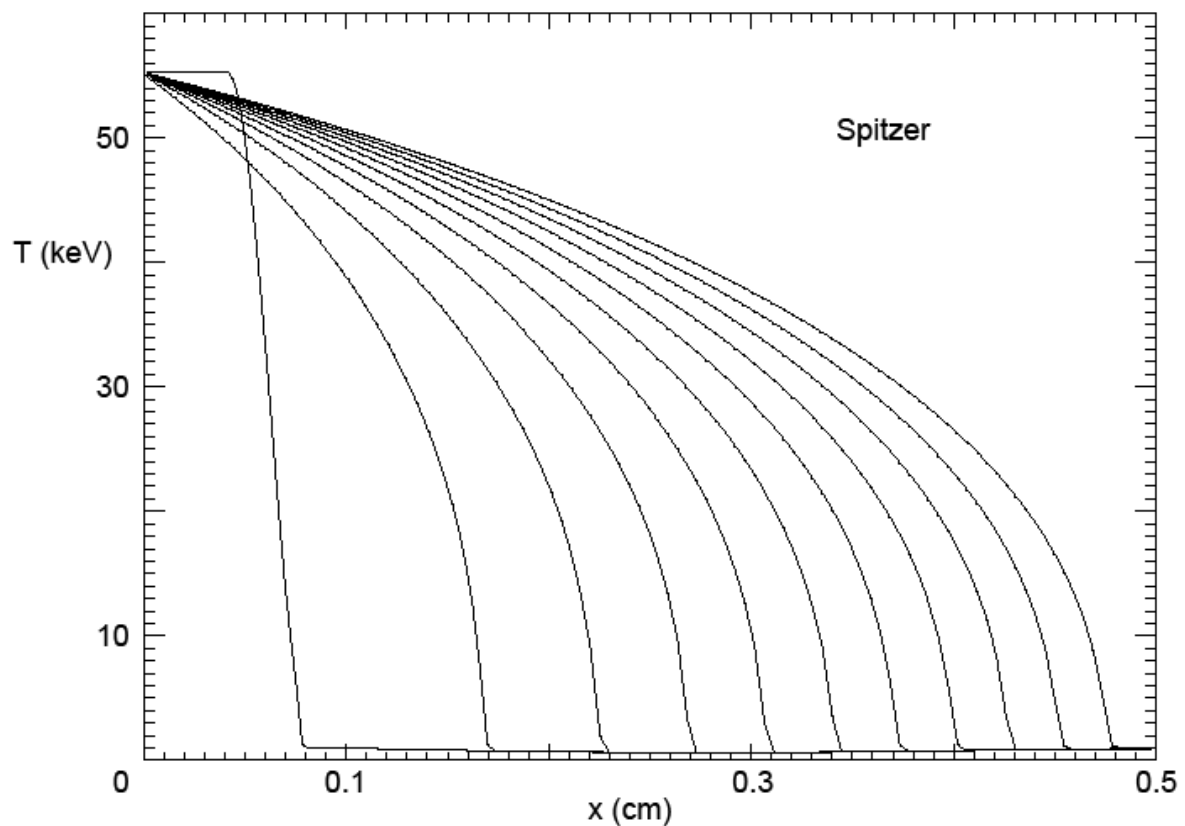


Fig.2

Equivalent diffusion model

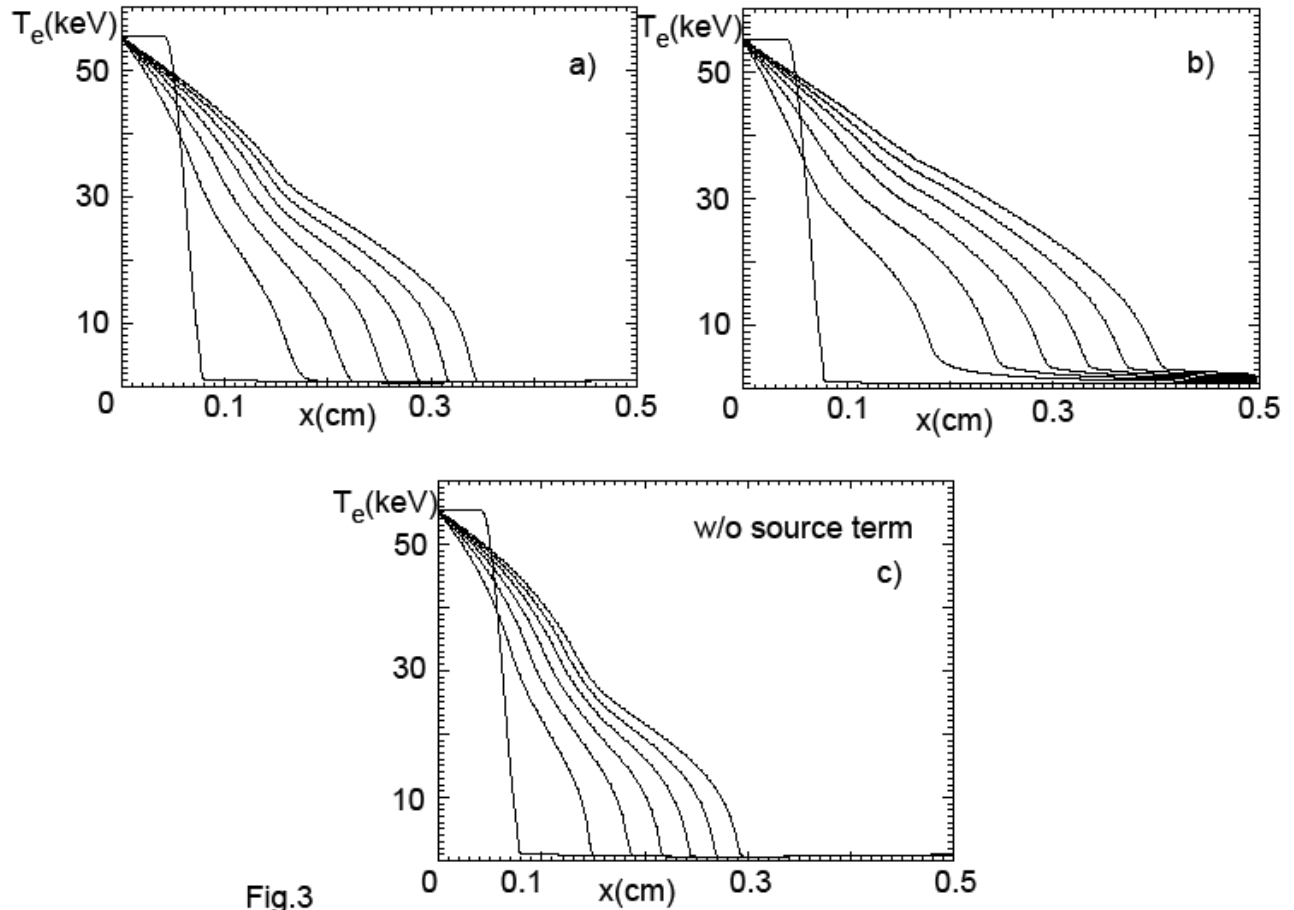


Fig.3

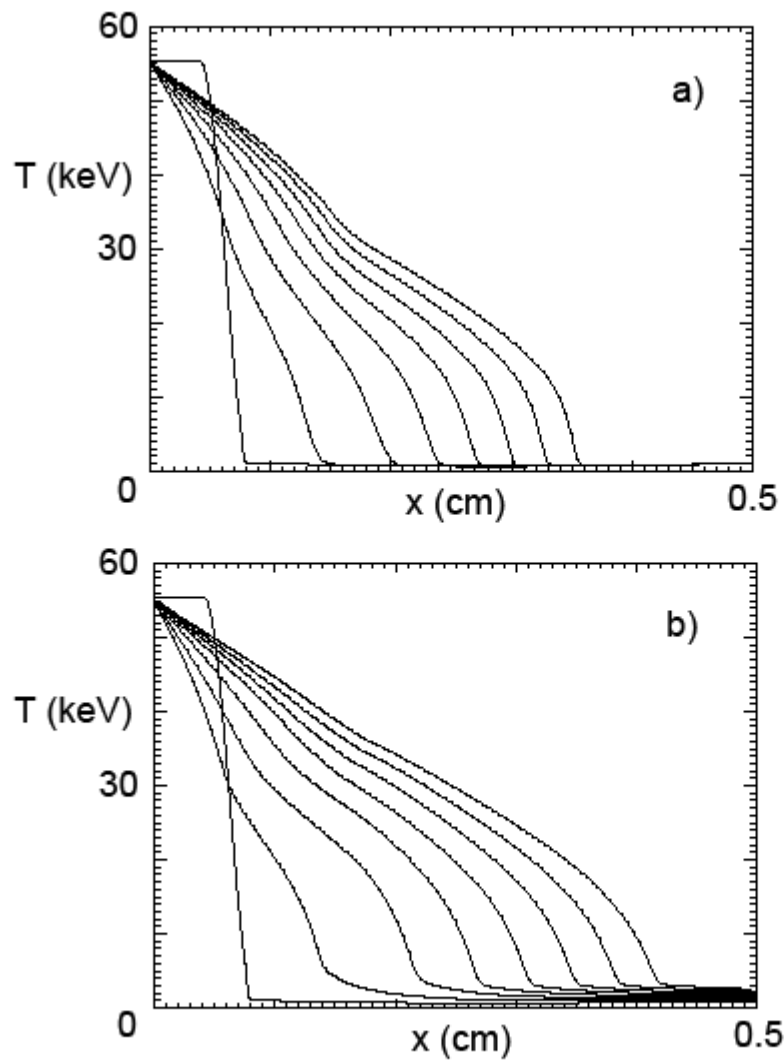


Fig.4

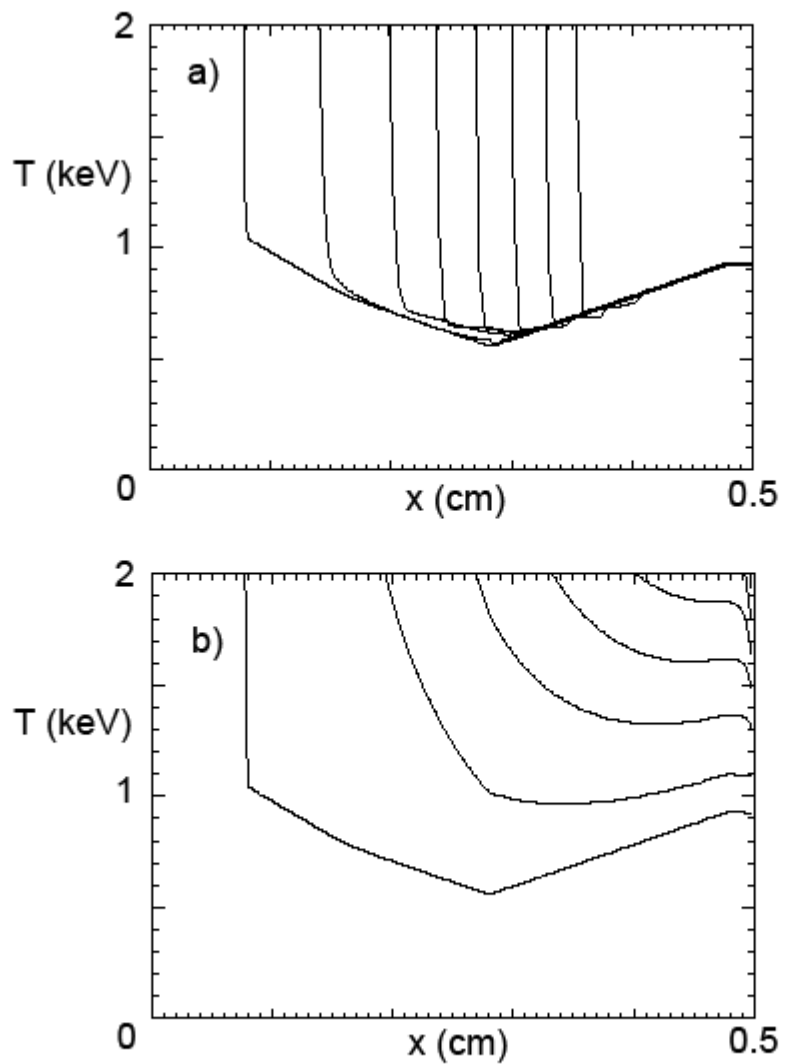


Fig.5

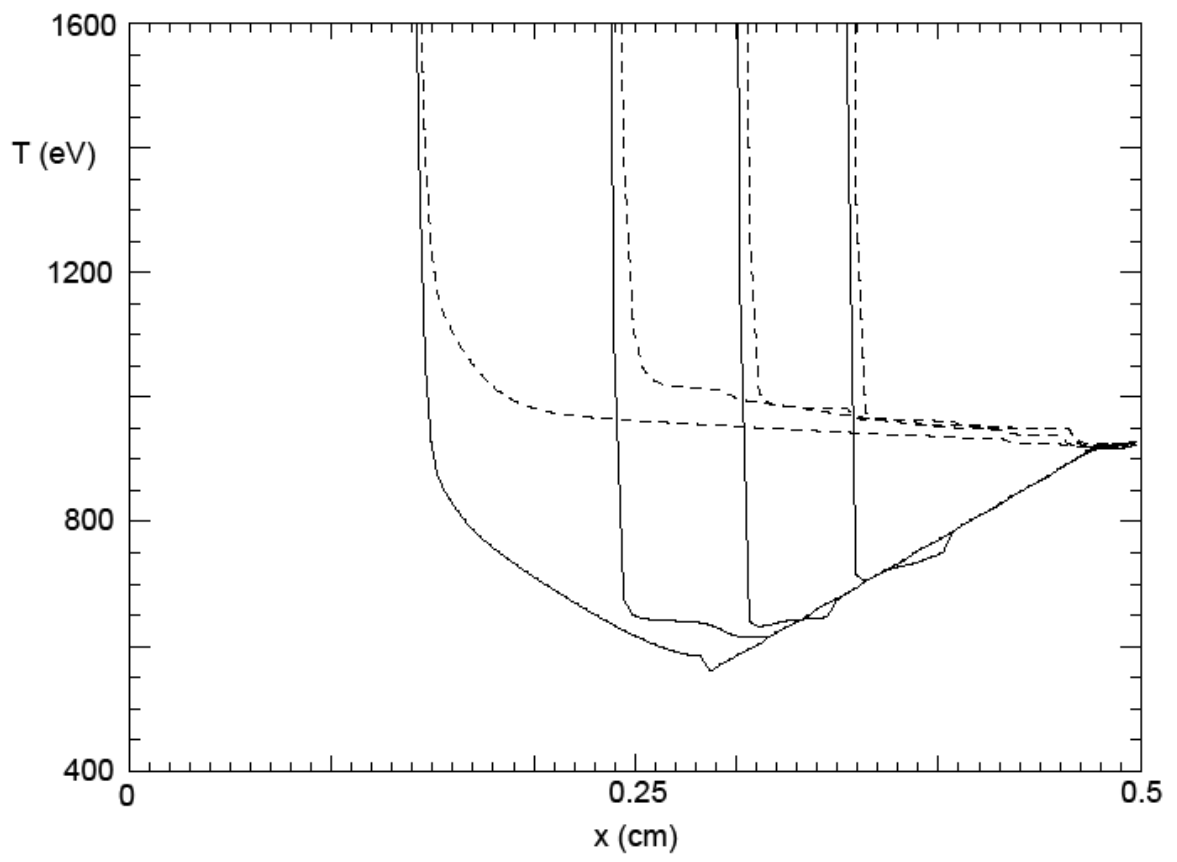
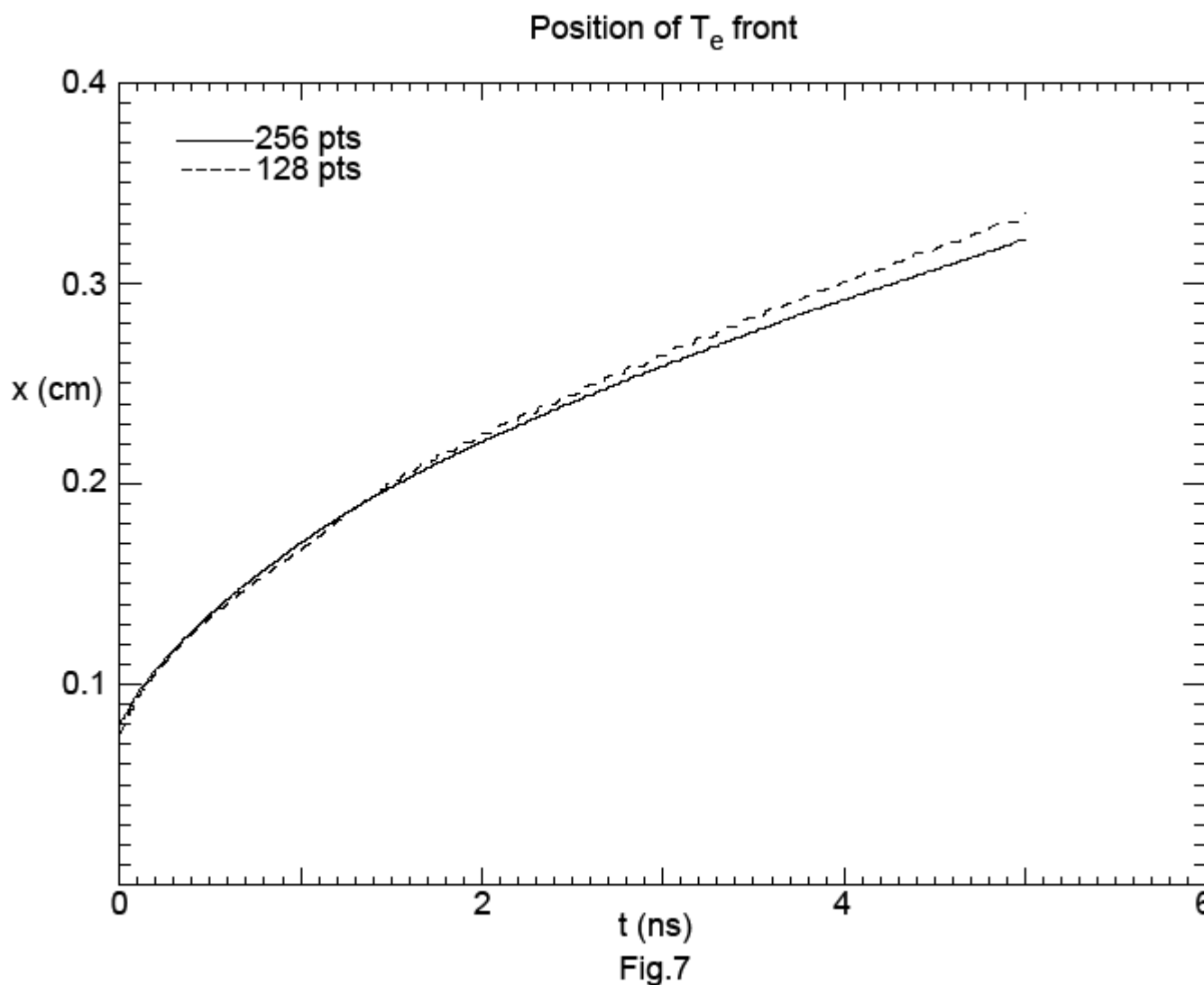


Fig.6



Comparison with Fokker-Planck solution
(Matte & Virmont)

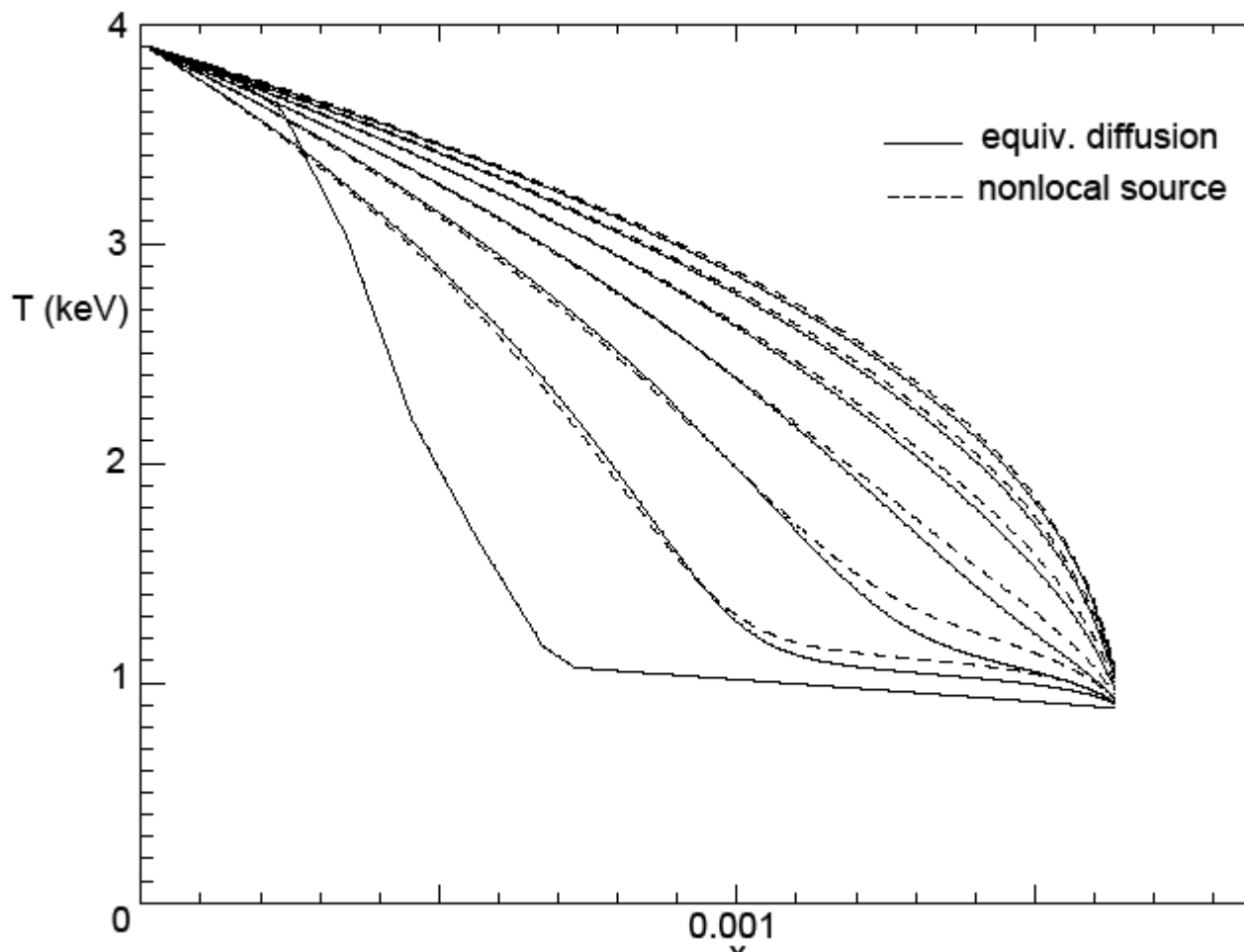


Fig.8

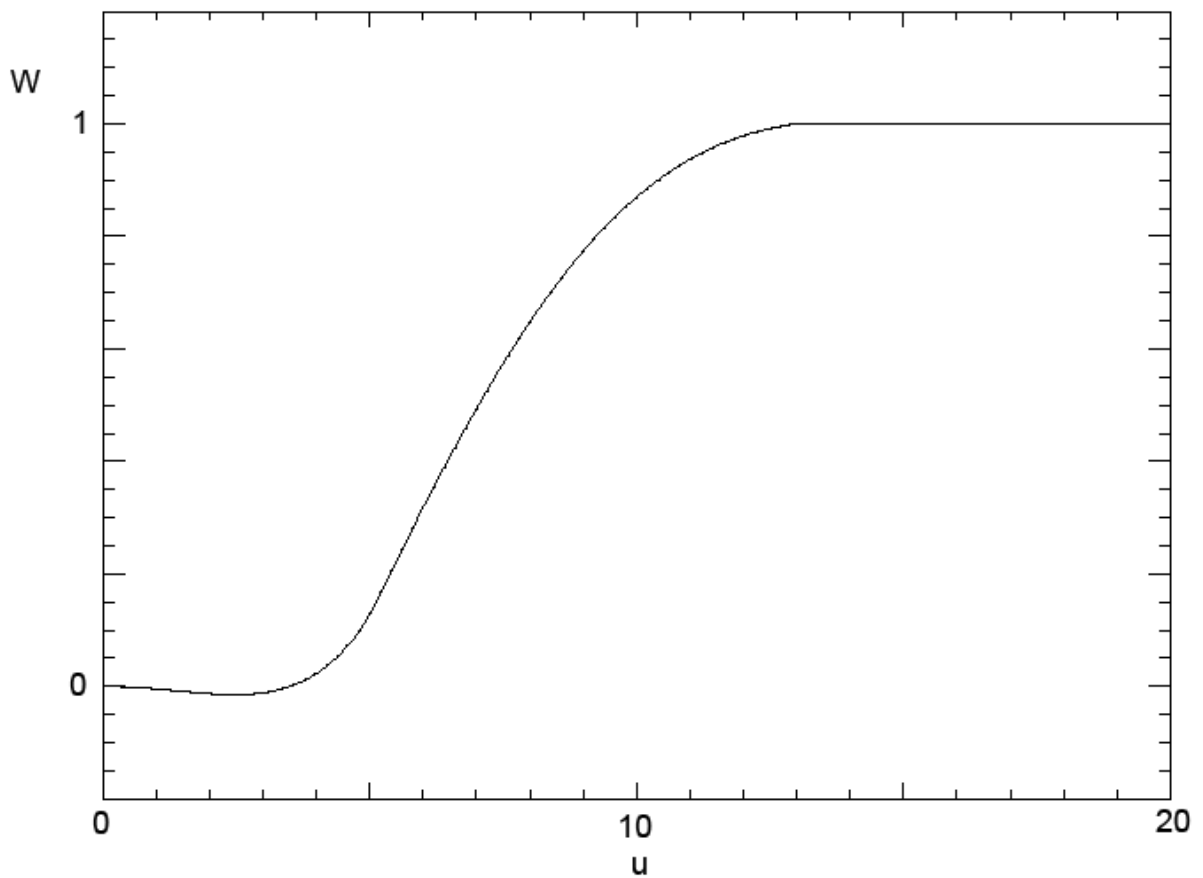


Fig.A1

